Transactions of the 15th International Conference on
Structural Mechanics in Reactor Technology (SMiRT-15)
Seoul, Korea, August 15-20, 1999

Simulation of the Dynamic Behavior of Steel Structures under Impact Loading

H.-J. Hilpert[1] and K. Willnow[2]

1) RWE Energie AG, Germany
2) Siemens AG, Power Generation Group (KWU), Germany

ABSTRACT
This paper presents an analytical technique based on the finite element method for determining the dynamic load-bearing behavior of linear thin-walled bars when subjected to impact loads from any direction. The theoretical basis for the method is the general theory of bending and torsion of thin-walled bars under consideration of shear deformation. The method accounts both for geometric non-linearities in the structure and for physical non-linearities in the material. The behavior at the contact point is idealized by means of a specially developed elasto-plastic contact spring.

The numerical algorithm is described by a step-by-step integration technique in the time domain.

1 INTRODUCTION

Columns and vertical bars of steel constructions in nuclear buildings are often placed close to planned breaks of piping and are thus exposed to the danger of impact by jet forces. The considerations of loading behavior in existing studies proceed from the assumption of an impact in the direction of the principle axis. At present idealized loading is usually applied for the design of loading capacity independent of its velocity and without consideration of a certain eccentricity along the principle axis.
Since the impact loading can act on the structural component from any direction a calculation model is developed on the basis of the Finite Element Method, which simulates the dynamic loading behavior of steel structures under spatial strain through impact.
The resistance of load-bearing steel structures such as columns or girders to impact loads must frequently be verified. Such loads may originate from vehicle impact in the case of columns which are located near roads, or may comprise loads imposed on support structures that are situated near predetermined breaking points in piping. Both cases result in impact-type dynamic loading of the thin-walled steel structure.

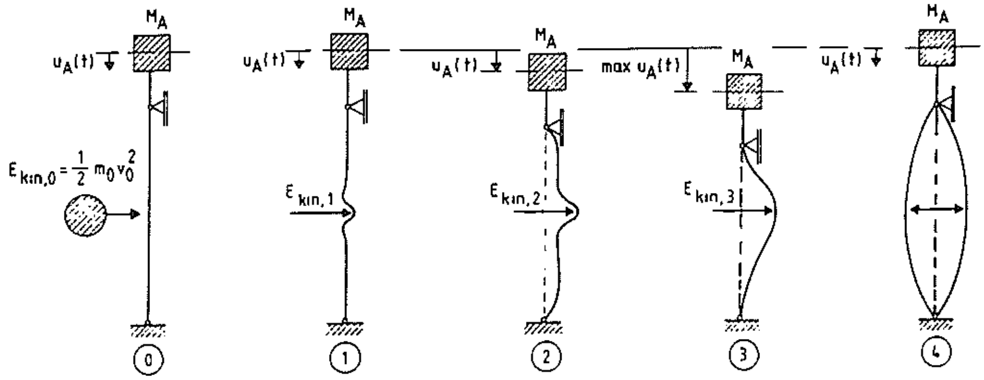

Figure 1 Load-Bearing Behavior of a Column Upon Impact Loading

The basic load-bearing behavior of a column which is subjected to transverse loading by a rigid mass m_0 at a velocity v_0 (Figure 1) can be divided into four phases:

Phase 1	Phase 2	Phase 3	Phase 4
Start of impact	Wave propagation	Vibration	Vibration decay

The most important conditions for describing the load-bearing behavior are phases 1 through 3. As the period under observation is very short, the contributions from structural damping are neglected in the analysis. Furthermore, it is assumed that the supported load represented by M_A always remains connected to the axis of the bar, i.e. there is no detachment.

2 LOAD-BEARING BEHAVIOR AT CONTACT POINT

The load on a system of bars that is induced by impact of a mass m_0 at velocity v_0 can be described in a dynamic analysis by means of a contact force. This contact force is determined by formulating the interaction between the impacting mass and the impacted mass using a contact force rule which is applied under consideration of the local and global deformation behavior of the bar system.

If one assumes that the impacting body is rigid, the approach distance $\Delta s(t)$ between the two bodies at the impact point $x = x_K$ can be described as the difference between the deformation of the contact point K and that of the reference point of the cross section B.

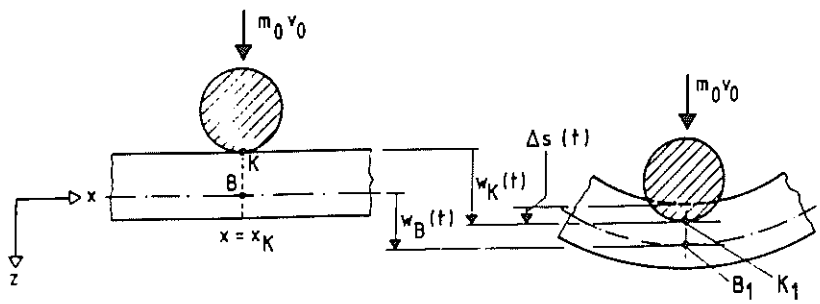

Figure 2 Deformation Behavior at Contact Point

Impact tests performed by Eibl and Feyerabend (1,2) on steel I-beams revealed nonlinear load-bearing behavior at the contact point with a large range of plastic flow typical for structural steel. Both the load-bearing behavior determined in the elastic range and the unloading from the plateau of plastic flow corresponded to the relationship known from Hertz (3).

Based on the experimental results, Feyerabend (2) proposed a contact force rule. This has been modified by Willnow (4,5) for numerical reasons to describe the nonlinear relationship between the contact force $F_K(t)$ and the approach distance between the two bodies $\Delta s(t)$. The derived elasto-plastic contact force rule is as follows:

- for the loading phase $$F_K(t) = \frac{K_K\, \Delta s(t)^p}{\left[1+\left(\frac{K_K\, \Delta s(t)^p}{\max F_K}\right)^n\right]^{\frac{1}{n}}} \qquad (1a)$$
- for the unloading phase $$F_K(t) = K_K \left(\Delta s(t) - \Delta s_{pl}\right)^q \qquad (1b)$$

3 LOAD-BEARING BEHAVIOR OF THIN-WALLED BAR

3.1 Displacement

A beam element with 7 degrees of freedom at each end i and j is employed $\vartheta^T = \{u(x), v(x), \varphi_z(x), w(x), \varphi_y(x), \vartheta(x), \psi(x)\}$ to simulate the three-dimensional deformation of a thin-walled bar,. In addition to the standard possibilities for translational and rotational deformation, ψ is used to represent twist, i.e. the relative rotation of the thin-walled sections of the bar.

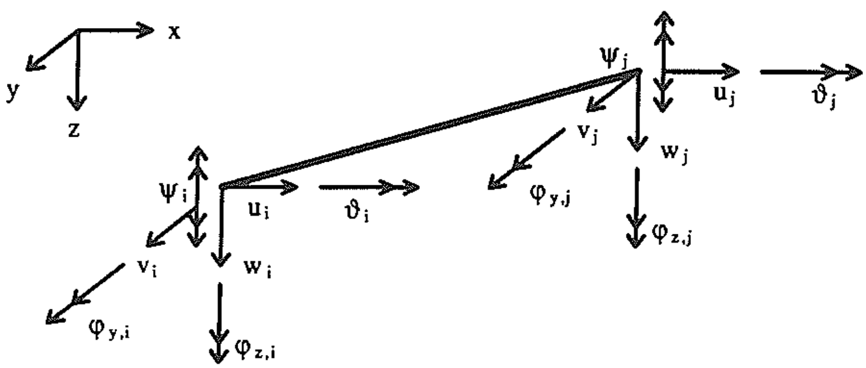

Figure 3 Degrees of Freedom of Beam Element

The shear effect is accounted for by an expanded deformation term based on Eq. (2) for each of the three coordinate directions of the bar. It is assumed that the shear deformations γ are approximately constant across the cross section.

$$\begin{aligned} \varphi_z &= v' + \gamma_z \\ \varphi_y &= -w' + \gamma_y \\ \psi &= \vartheta' + \gamma_\omega \end{aligned} \qquad (2)$$

Deformation of the bar axis is determined by the finite element method, in which the position of the reference axis can be chosen arbitrarily. The standard rule

$$\vec{v} = \underline{N}\,\vec{u} = (\underline{I}\,\underline{N}_i, \underline{I}\,\underline{N}_j) \begin{Bmatrix} \vec{u}_i' \\ \vec{u}_j \end{Bmatrix} \tag{3}$$

is employed to couple the nodal variables of vector $\vec{u}$ with the displacement functions of vector $\vec{v}$. Matrix $\underline{N}$ represents the shape functions multiplied by the unit matrix $\underline{I}$.

3.2 Distorsion

Assuming that the overall contour of the cross section does not change during deformation, the displacement and hence the distortion of each point on the cross section can be described solely by the deformation of the reference axis.

The distortion is coupled to the deformation by the differential operator $\underline{B}$ or, for nonlinear distortion, by $\underline{B}$(u) which is a function of the deformation.

$$\begin{aligned} \vec{\varepsilon} &= \vec{\varepsilon}_l + \vec{\varepsilon}_{nl} &&= \underline{B}\,\vec{u} + \frac{1}{2}\underline{B}(\vec{u})\,\vec{u} &&= \underline{L}\,\underline{N}\,\vec{u} + \frac{1}{2}\underline{L}(\vec{u})\,\underline{N}\,\vec{u} \\ \delta\vec{\varepsilon} &= \delta\vec{\varepsilon}_l + \delta\vec{\varepsilon}_{nl} &&= \underline{B}\,\delta\vec{u} + \underline{B}(\vec{u})\,\delta\vec{u} &&= \underline{L}\,\underline{N}\,\delta\vec{u} + \underline{L}(\vec{u})\,\underline{N}\,\delta\vec{u} \end{aligned} \tag{4}$$

Apart from translational and rotational deformation components, the linear and nonlinear distortion components of vectors $\vec{\varepsilon}_l = \left\{e_{xx}, g_{xy}, g_{xz}\right\}_l$ and $\vec{\varepsilon}_{nl} = \left\{e_{xx}, g_{xy}, g_{xz}\right\}_{nl}$ in Eq.s (5) and (6) also contain warping components which lead both to bar elongation (strain) and to shear distortion. The description of Eq. (6) is derived from the theory of moderately large deformations.

$$\begin{aligned} e_{xx,l} &= u' - \varphi_z'\,y + \varphi_y'\,z + \psi'\omega \\ g_{xy,l} &= v' - \varphi_z - \vartheta' z - \psi\frac{\partial\omega}{\partial y} \\ g_{xz,l} &= w' + \varphi_y + \vartheta' y - \psi\frac{\partial\omega}{\partial z} \end{aligned} \tag{5}$$

$$\begin{aligned} e_{xx,nl} &= \frac{1}{2}\left(v'^2 + w'^2\right) + \frac{1}{2}\vartheta'^2\left(y^2 + z^2\right) + \vartheta\left(\varphi_y'\,y + \varphi_z'\,z\right) + \vartheta'\left[\left(w' + \varphi_y\right)y + \left(-v' + \varphi_z\right)z\right] \\ g_{xy,nl} &= -u'\left(\varphi_z + \psi\frac{\partial\omega}{\partial y}\right) + \left(w' + \varphi_y\right)\vartheta - \varphi_y'\,\psi\frac{\partial\omega}{\partial y}z \\ g_{xz,nl} &= u'\left(\varphi_y - \psi\frac{\partial\omega}{\partial z}\right) + \left(-v' + \varphi_z\right)\vartheta + \varphi_z'\,\psi\frac{\partial\omega}{\partial z}y \end{aligned} \tag{6}$$

3.3 Stress

The distortions $d\vec{\varepsilon} = \left\{de_{xx}, dg_{xy}, dg_{xz}\right\}$ are coupled with the stresses $d\vec{\sigma} = \left\{d\sigma_{xx}, d\tau_{xy}, d\tau_{xz}\right\}$ using the elasto-plastic rule for materials.

$$d\vec{\sigma} = \underline{C}^{ep}\, d\vec{\varepsilon} \tag{7}$$

On account of the thin-walled sections, only the shear stress component τ_{xs} is obtained in the plane defined by the bar axis and the section centerline. The differential increases in the stress components are thus obtained using Eq. (8).

$$d\vec{\sigma} = \begin{Bmatrix} d\sigma_{xx} \\ d\tau_{xs} \end{Bmatrix} = \begin{bmatrix} \dfrac{E\left(1-3\beta\,\sigma_{xx}^2\right)}{1-\beta\,\sigma_{xx}^2(1-2\nu)} & -\dfrac{E\cdot 3\beta\,\sigma_{xx}\tau_{xs}}{1-\beta\,\sigma_{xx}^2(1-2\nu)} \\ -\dfrac{E\cdot 3\beta\,\sigma_{xx}\tau_{xs}}{1-\beta\,\sigma_{xx}^2(1-2\nu)} & G\left[1-\dfrac{9\beta\,\tau_{xs}^2}{1-\beta\,\sigma_{xx}^2(1-2\nu)}\right] \end{bmatrix} \begin{Bmatrix} de_{xx} \\ dg_{xs} \end{Bmatrix} \tag{8}$$

where $\beta = \dfrac{1}{3+\dfrac{E_T\,2(1+\nu)}{E-E_T}}\cdot\dfrac{1}{f_{y,dyn}}$ for plastic material behavior, otherwise $\beta = 0$.

In the case of impact-type loading of structural steel, the material strength increases significantly as a function of strain rate. This dynamic behavior is accounted for in the yield strength of the structural steel by the Cowper-Symonds-Bodner rule in accordance with Eq. (9) using the parameters from Perzyna (6). The material curve is idealized as a bilinear stress-strain relationship in the numerical algorithm.

$$f_{y,dyn} = f_{y,stat}\left[1+\left(\frac{\dot{\varepsilon}}{40}\right)^{\frac{1}{5}}\right] \tag{9}$$

3.4 Principle of Virtual Work

As the internal and external work in the system must always be in equilibrium, the energy balance of the system can be described with the aid of a virtual deformation condition.

$$\int_V \delta\bar{\varepsilon}_l^T\,\bar{\sigma}\,dV + \int_V \delta\bar{\varepsilon}_{nl}^T\,\bar{\sigma}\,dV + \int_V \delta\bar{v}^T\rho\ddot{\bar{v}}\,dV - \int_V \delta\bar{v}^T\,\bar{p}\,dV = \delta\vec{u}^T\,\vec{f} \tag{10}$$

The Eq. for virtual internal work and virtual external work is obtained in matrix form by combining Eq.s (2) through (7) and Eq. (10).

$$\delta\vec{u}^T\left\{\int_V \underline{B}^T\,\underline{C}^{ep}\,\underline{B}^T\,\vec{u}\,dV + \int_V \underline{B}(u)^T\,\underline{C}^{ep}\,\underline{B}^T\,\vec{u}\,dV + \int_V \underline{N}^T\rho\,\underline{N}\,\ddot{\vec{u}}\,dV\right\} = \delta\vec{u}^T\left\{\vec{f} + \int_L N^T\bar{p}\,dx\right\} \tag{11}$$

As all of the virtual expressions have C^0 continuity, only linear functions are used to describe the displacements and rotations in forming the element matrices. A reduced integration of the shear stiffness components is carried out to prevent shear locking.

4 NUMERICAL ANALYSIS OF SYSTEM RESPONSE

The system responses are analyzed in the time domain using an implicit time integration method. A nonlinear load-bearing behavior is obtained due to plastic deformation in the bar system and the associated decreased stiffness. Iteration is required since the equilibrium conditions are then no longer fulfilled within the time steps. This equilibrium iteration by the standard Newton-Raphson method is used to adjust the system stiffness to the instantaneous plastic condition. The resulting unbalanced forces are accounted for as additional loads on the load side. The iteration is continued until the unbalanced loads are sufficiently small.

4.1 Modeling

In the center of the analysis a fiber plane model with beam elements based on the finite element method is used for the numerical simulation taken into account the physical non-linearities by the elasto-plastic material. In this model, the cross section consists of individual sections (planes) which are further divided into individual fibers. The elasto-plastic material behavior of the bar is accounted for within the iteration process by the residual load-carrying potential of the cross section.

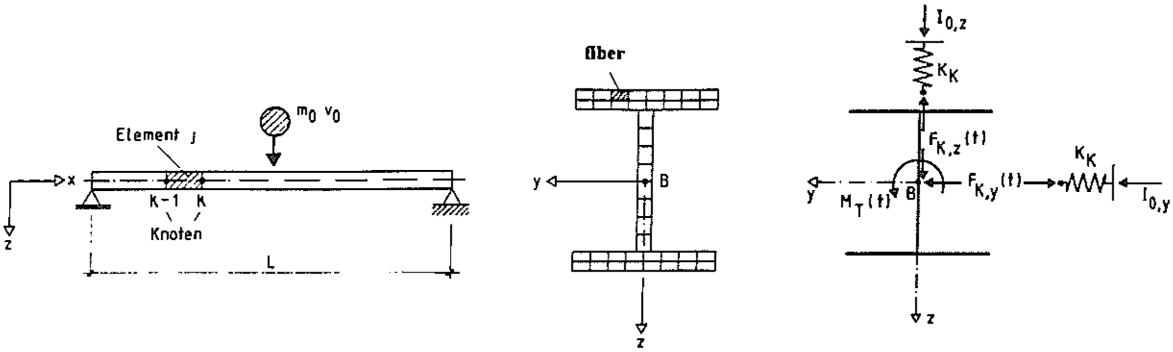

Figure 4 Idealized System of the Cross Section in Fiber Plane Model and the Contact Point

The distortion condition is obtained for each fiber at each point in time. This allows determination of the stress condition based on von Mises' flow rule. If the stress intensity calculated from the normal and shear stress is above the dynamic yield strength of Eq. (9), the excess stress is applied to the yield surface using the differential elasto-plastic material rule according to Eq. (8).

Since the impact can act on the bar system as a three-dimensional load, spring-mass systems are coupled to the finite element model of the bar system to idealize transverse deformation in the y and z directions. In addition, the offset of the contact point from the reference point of the cross section must be accounted for by an external torsional moment (Figure 4).

The deformation components required to calculate the approach distance between the two bodies are determined from the equilibrium analysis of the spring-mass system. On the other hand, the system responses of the bar system are determined from the analysis of the overall system. Since the loading of the bar system in terms of the contact force is not known at the start of each time step Δt, an iteration is performed in the finite element analysis in each such time step. The elasto-plastic relationship of Eq. (1) is used as the contact force rule.

4.2 Application

The Figures 5 and 6 show two examples how the numerical algorithm can be used for the evaluation of system responses. In both cases a hard contact force caused by an impact is acting on a steel structure. Figure 5 show a strong vehicle like a fork lift impacting a steel column and Figure 6 gives an idea how a jet force coming from a broken pipe above strengthen a steel beam.

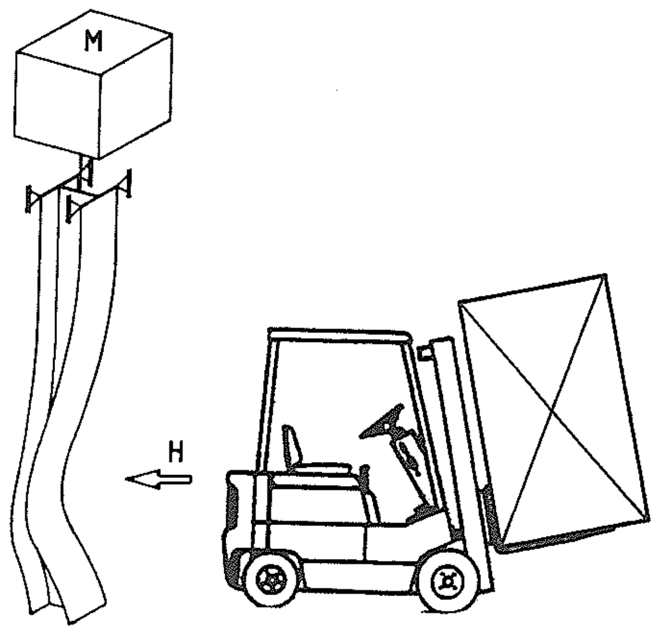

Figure 5 Impact of a Steel Column by a Fork-Lift

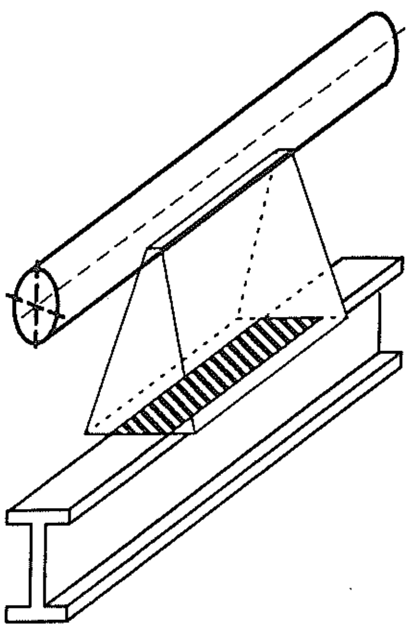

Figure 6 Impact of a Steel Beam by Jet Forces

In case of standard steel beams the contact conditions mainly concerning the maximum contact force $maxF_K$ and the spring constant K_K in Eq. (1) can be assume as

$$maxF_K \approx 1100kN$$
$$K_K \approx 25000kN/cm^{3/2}$$

The numerical parameter p and q can be set to 1.7 with the parameter n=8. The time step has to be set very small simulating the contact force sufficiently.

5 CONCLUSION

The numerical model presented above can be used to simulate the load-bearing behavior of thin-walled bar systems under three-dimensional dynamic impact loading. Comparison of the calculated and measured system responses of a steel column demonstrates that the rules applied with regard to member kinematics, the description of the dynamic material behavior and the use of a subsystem for the contact point yield good results.

6 REFERENCES

(1) Book

1. Eibl, J.; Feyerabend, M.: Final report on research project *Stoßbelastung von normalkraftbeanspruchten stabförmigen Tragwerksteilen aus Stahl, Holz und Stahlbeton,* Institut für Massivbau und Baustofftechnologie Abt. Massivbau, Karlsruhe University, 1984
2. Feyerabend, M.: *Der harte Querstoß auf Stützen aus Stahl und Stahlbeton,* doctoral thesis, Karlsruhe University, 1987

(2) Paper in a Journal

3. Hertz, H.: "Über die Berührung fester elastischer Körper", *Journal für reine und angewandte Mathematik 32 (1862), pp. 237-376*

(3) Book

4. Willnow, K.: *Stahlstützen unter räumlicher dynamischer Beanspruchung durch Anprall,* series of publications by the Lehrstuhl für Stahl- und Verbundbau der Ruhr-Universität Bochum, Germany, Volume 1 (1996)

(4) Paper in Conference Proceedings

5. Willnow, K.: "Simulation des Tragverhaltens von Stahlstützen unter räumlicher dynamischer Beanspruchung durch Anprall, Dynamische Probleme - Modellierung und Wirklichkeit-", *Report of the Curt-Risch Institute at the University of Hanover, 1996, Volume of Proceedings pp. 281-300*

(5) Paper in a Journal

6. Perzyna, P.: "On fading memory of a material", Archives of Mechanics, Polish Academy of Science, *Inst. of Fundamental Technological Research 19 (1967), 537-547*